Available online at www.sciencedirect.com
ScienceDirect
International Journal of Heat and Fluid Flow 28 (2007) 882–893
International Journal of HEAT AND FLUID FLOW
www.elsevier.com/locate/ijhff

The thermal characteristics of a hot wire in a fluctuating freestream flow

W.Z. Li [a], B.C. Khoo [a,b,*], D. Xu [c]

[a] Department of Mechanical Engineering, National University of Singapore, Kent Ridge, Singapore 119260, Singapore
[b] Singapore-MIT Alliance, 4 Engineering Drive 3, Singapore 117576, Singapore
[c] Institute of High Performance Computing, 1 Science Park Road, #01-01 The Capricorn, Singapore Science Park II, Singapore 117528, Singapore

Received 2 June 2005; received in revised form 12 October 2006; accepted 14 November 2006
Available online 2 February 2007

Abstract

A two-dimensional numerical study is carried out to obtain the thermal response of a hot wire in a fluctuating freestream flow. The ranges of the parameters considered in this study are $0.025 \leqslant Re \leqslant 200$, $0 \leqslant Sc$ (non-dimensional frequency) $\leqslant 0.32$ and A (dimensionless amplitude of the imposed streamwise velocity pulsation) $\leqslant 0.6$. The results showed that for a fluctuating flow, a typical hot wire having been calibrated under imposed mean free stream condition can be employed for velocity measurement in the typical operating range of $Re \approx O(1)$ or smaller. The very rapid thermal response of the hot wire has enabled the faithful measurement of fluctuating velocity in the typical range of frequency of up to O(10) kHz and amplitude range of $A \leqslant 0.4$ encountered in a turbulent flow.

Keywords: Hot-wire; Fluctuating flow; Free stream; Thermal response

1. Introduction

Despite the progress made and success of particle image velocimetry (PIV) and of laser Doppler anemometry (LDA) for velocity measurements, hot-wire anemometry (HWA) still remains the workhorse for turbulent flow measurements for many researchers. Hot-wire anemometry provides not only high spatial resolution of the velocity field but also (supposedly) fast response due to its small size of active element (micrometers in diameter) and corresponding low thermal inertia. Hot-wire anemometry has become a well-established measuring technique widely used to obtain local, time-resolved information on fluid velocity fields in experimental fluid mechanics.

The response of a hot-wire anemometer can and should be determined by subjecting it to an accurately known fluctuating velocity and then observing the output. Such comparison provides the user with information on the dynamic response of the said hot wire which is then used to validate or track an unknown unsteady flow; it can also be used to check on the hot-wire manufacturer's stated specifications on the instrument response. However, it is not trivial experimentally to generate an accurately known fluctuating velocity field to obtain the true dynamic response. To a large extent the user has invariably relied solely on the manufacturer's specification which is obtained via the standard electronic perturbation tests to determine the cut-off frequency and taken synonymously as the dynamic response frequency of the hot-wire sensor; this is not necessarily so (see Khoo et al., 1999). Strictly, a hot-wire anemometer should first be calibrated in a known flow (usually a steady flow) and then subsequently subjected to imposed fluctuating flow with known amplitude and frequency. In this way, the output of the hot wire via the calibration curve can be compared directly to the imposed fluctuating flow to determine the overall response of the hot-wire system. One may also consider a dynamic calibration as opposed to the commonly employed static calibration where the imposed flow is steady.

* Corresponding author. Tel.: +65 68742889; fax: +65 67791459.
E-mail address: mpekbc@nus.edu.sg (B.C. Khoo).

0142-727X/$ - see front matter © 2006 Elsevier Inc. All rights reserved.
doi:10.1016/j.ijheatfluidflow.2006.11.005

Nomenclature

A	dimensionless amplitude of the imposed streamwise velocity pulsation
C_d	drag coefficient
D	diameter of hot wire
Ec	Eckert number $= \frac{U_0^2}{C_p(T_w - T_\infty)}$
f	imposed or pulsating frequency of the incoming fluctuating flow
f_{imp}	imposed pulsating frequency of the incoming flow
f_{DV}	dynamic response of the hot-wire system in the form of the cut-off frequency obtained from imposed velocity perturbation test
f_{DS}	dynamic response of the hot-wire system in the form of the cut-off frequency obtained from square wave electronic perturbation test
f_s	vortex shedding frequency
f_v	natural Strouhal frequency in the unforced (unperturbed) wake
Gr	Grashof number $= \frac{g\beta(T_w - T_\infty)D^3}{\upsilon_\infty^2}$
H'	heat flux through the closed circulation which surrounds the cylindrical hot wire
L	hot-wire length
Nu	Nusselt number
Nu_0	Nusselt number at (imposed) uniformed flow condition
N_{uf}	Nusselt number based on film temperature
Pe	Peclet number $= RePr$
Pr	Prandtl number $= \frac{\mu_\infty Cp_\infty}{k_\infty}$
Re	Reynolds number $= \frac{U_0 D}{\upsilon_\infty}$
Re_f	Reynolds number based on fluid properties at the film temperature
S	Strouhal number which is used as a non-dimensional quantity to describe the vortex shedding frequency $S = \frac{D}{\tau_s U_\infty}$
Sc	non-dimensional frequency, $Sc = \frac{f}{f_0} = \frac{fD^2}{Re\upsilon_\infty}$, of the imposed streamwise fluctuation
t	time
T	temperature
U_0	the true upstream incoming flow velocity at the location of hot-wire center

Greek symbols

ε	dimensionless of imposed fluctuation $\varepsilon \equiv \Delta u/(2\pi f d)$
μ	dynamic viscosity
υ	kinematic viscosity
ω	frequency of the pulsation
τ	overheat ratio of the hot wire, $\tau \equiv T_w/T_\infty$
τ_s	period of the vortex shedding
∞	at the inlet of computational domain

A dynamic calibration method was previously applied by Perry and Morrison (1971) who developed it into a somewhat fairly standard calibration procedure. The procedure calibrates the hot wire (dynamically) by shaking the probe in a uniform air flow of known velocity, thereby subjecting the wire to a known velocity fluctuation. However, probably due to the complex and low frequency limitation of the dynamic calibration involved, the calibration of Perry and Morrison (1971) was only carried out in a known small sinusoidal motion in the low frequency range from 0 to 10 Hz, which may be deemed too low for application to most turbulent flow measurements. A majority of researchers still resort to static calibration methods based on the underlying (implicit) assumption that the hot wire can faithfully follow a fluctuating flow due to its small size of active element and hence small thermal inertia.

In this work, it is the intention to investigate numerically the thermal response of a hot wire subjected to an imposed fluctuating flow. Because the response of the electronic system in the anemometer is invariably much better than the physical thermal response, our findings of the thermal response of the hot wire should reveal the overall response and sensitivities of the hot-wire system. From Li (2004), it is found that the "...the cut-off frequency of the system is mainly controlled by the hot wires rather than the anemometer itself, provided that the cut-off frequency of the latter is reasonably high...", which concurs with the series of experimental findings of Khoo et al. (1998, 1999) and Chew et al. (1998a) that the dynamic response of the hot-wire system in the form of the cut-off frequency due to imposed velocity perturbation test (f_{DV}) is about one to five order of magnitude lower than the square wave electronic perturbation test given as f_{DS}, depending on whether it is the hot wire or hot film. The experiments *indirectly* support the contention that the thermal response of the hot wire is the overriding factor for determining the overall response of the hot-wire system and not the (electronic) CTA unit per se.

Kezios and Prasanna (1966), Saxena and Laird (1978), Leung et al. (1981) and Cheng et al. (1997a,b) have conducted extensive experimental and numerical studies to investigate the effect of the transverse oscillation of a cylinder on forced convection. They set a cylinder to oscillate transversely in the direction normal to the flow stream, and found that nonlinear interaction occurs particularly as the cylinder oscillation frequency gradually approaches the natural frequency of vortex shedding. Because a hot wire is usually employed to measure the velocity in the horizontal/streamwise direction, these findings may not have much direct bearing on the response of hot wire to a fluctuating flow in the streamwise direction. Furthermore as the hot-wire diameter employed is usually in micron size,

the typical Reynolds number encountered in most flow application is well below the critical value where vortex shedding begins.

Other works which set the cylinder to oscillate transversely in the direction normal to the flow stream include the experiments by Honji (1981), Bearman et al. (1985), Obasaju et al. (1988) and Skomedal et al. (1989), and numerical investigations by Smith and Stansby (1991), Justesen (1991) and Iliadis and Anagnostopoulos (1998). Iliadis and Anagnostopoulos placed the cylinder in an oscillatory flow in order to study the oscillation effect on forced convection. Unfortunately, most of these works only focused on the variation of the flow field around the cylinder due to the imposed oscillatory flow. Much less attention is directed on the associated thermal convection surrounding the cylinder.

Of the few studies carried out on the heat transfer from a cylinder subjected to a streamwise oscillatory flow, Hegge Zijnen (1958) is probably one of the first to conduct such experiments in this area. He found that for low values of Reynolds number (less than 5) the (averaged) heat transfer rate from a tungsten wire undergoing vibrations in the direction of airflow decreased from the static value. Apelt and Ledwich (1979) in their numerical simulation found that there is an increase of amplitude of computed Nusselt number for the hot-wire cylinder in a streamwise fluctuating flow compared to the steady state value associated with the instantaneous value of Reynolds number (referred to as the 'quasi-steady' response curve). Their calculations were unfortunately carried out only for a single case of relatively high $Re = 10$. In more recent times, Gundappa and Diller (1991) reported on the time-averaged local distributions of heat transfer around a heated cylinder placed in a turbulent and pulsating cross flow. However, the Reynolds number investigated was very much higher than the typical Reynolds number encountered by a hot wire in its operation. As a result, there is still a dearth of knowledge on the heat transfer from a cylinder in a streamwise pulsating flow of reasonably high frequencies and at the lower range of Reynolds number. As hot-wire anemometry has and continues to play an important role for the measurement of velocity in turbulent flows, it is necessary to conduct more detailed studies on the responses and performance of hot-wire operation in a fluctuating flow. This observation serves as a further motivation for our present investigation of the heat transfer characteristic of the hot wire operating in a fluctuating flow as in a turbulent flow measurement.

This work aimed to find the heat transfer response of a cylinder (hot wire) in a pulsating flow by solving the Navier–Stokes equation coupled with the energy equation using a control volume method. The ranges of the parameters considered in this study are $0.015 \leqslant Re \leqslant 200$ with a distinct emphasis on the low Re regime where the typical hot wire operates, $0 \leqslant Sc \leqslant 0.32$ and $A \leqslant 0.6$. Here $Re \equiv \frac{U_0 D}{\upsilon_\infty}$ (Reynolds number based on the wire diameter and mean upstream velocity), $Sc \equiv \frac{fD^2}{Re\upsilon_\infty}$ (a non-dimensional frequency of the imposed streamwise velocity frequency) and A is the dimensionless amplitude of imposed streamwise velocity fluctuation.

2. Governing equations and boundary conditions

The following assumptions and considerations are adopted in the numerical analysis:

1. It is an unsteady, incompressible, 2-D laminar flow with heat transfer past an infinitely long circular wire that is aligned normal to the flow.
2. The wire is subjected to an imposed streamwise pulsating velocity field.
3. The viscosity and thermal conductivity are treated as temperature dependent. The body force is accounted for as in the Boussinesq assumption.
4. Natural convection and viscous heating are included, and the direction of gravity is in the vertical direction and perpendicular to the oncoming flow.

It may be mentioned that some recent works like Shi et al. (2004) have argued that the compressibility effect of non-constant density be included by treating density as varying with temperature but still independent of pressure. Their work has shown among various results some differences of the computed Nusselt number for a heated cylinder in a flow where full dependence of the fluid properties is accounted for versus where the density is kept constant but viscosity is temperature dependent. The differences, however, indicate a decreasing trend from about 8% to 6% as Re decreases from 148.3 to 29.6 (see their Table 3). This observation, coupled with the recent incompressible flow calculation in Li et al. (2006) for the hot wire placed near the wall which agreed well with the experimental results of Chew et al. (1998a) and Krishnamoorthy et al. (1985), suggest that the effect where density is not treated as a constant is likely to be of secondary importance especially for the operating conditions of a hot wire at low Re and low Mach number. On the other hand, the work of Shi et al. has clearly indicated the critical importance of temperature dependent viscosity.

The schematic drawing of pulsating flow past a cylinder in the computational domain is depicted in Fig. 1. Boundary $B1$ is the inflow boundary, $B2$ is the top boundary, $B3$ is the bottom boundary, $B4$ is the outflow boundary and boundary $B5$ is on the surface of the hot wire. H is the distance between the top boundary ($B2$) and bottom boundary ($B3$). Based on the need for domain size independence (Section 3), a domain extending $650D$ from the wire in four directions is implemented; correspondingly, H is $1300D$.

Taking the diameter of the hot wire D as the characteristic length, the upstream mean velocity at the wire location (U_0) as the characteristic velocity, the characteristic time is D/U_0 and the following dimensionless variables (as indicated by '*') result,

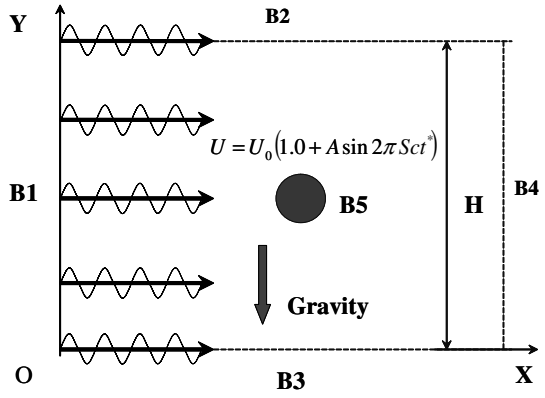

Fig. 1. Schematic drawing of the computational region.

$$x^* = \frac{x}{D}, \quad u^* = \frac{u}{U_0}, \quad p^* = \frac{p}{\rho_\infty U_0^2}, \quad T^* = \frac{(T - T_\infty)}{(T_w - T_\infty)},$$
$$\mu^* = \frac{\mu}{\mu_\infty}, \quad K^* = \frac{K}{K_\infty}.$$

Here the subscript '∞' denotes the condition at the upstream location and the dimensional variables take on the usual meaning. The non-dimensionalised governing equations of continuity, momentum and energy can be expressed respectively as follows,

Continuity equation:

$$\frac{\partial}{\partial x_i^*}(u_i^*) = 0 \quad i = 1, 2 \tag{1}$$

Momentum equations:

$$\frac{\partial}{\partial t^*}(u_i^*) + u_i^* \frac{\partial}{\partial x_i^*}(u_j^*) = -\frac{\partial p^*}{\partial x_j^*} + \frac{1}{Re}\frac{\partial}{\partial x_i^*}\left[\mu^*(T^*)\frac{\partial u_j^*}{\partial x_i^*}\right] + \left(\frac{Gr}{Re^2}\right)T^* \quad i, j = 1, 2 \tag{2}$$

Energy equation:

$$\frac{\partial}{\partial t^*}(T^*) + \frac{\partial}{\partial x_i^*}(u_i^* T^*) = \left(\frac{1}{Re * Pr}\right)\frac{\partial}{\partial x_i^*}\left[k^*(T^*)\frac{\partial T^*}{\partial x_i^*}\right] + \frac{Ec}{Re}\cdot \Phi^* \quad i = 1, 2 \tag{3}$$

Here u_i and x_i are the Cartesian velocity components and coordinates, respectively. The dissipation function is

$$\Phi^* = \left(\frac{\partial u_i^*}{\partial x_j^*} + \frac{\partial u_j^*}{\partial x_i^*}\right)\frac{\partial u_i^*}{\partial x_j^*} \tag{4}$$

where μ^* is the dimensionless dynamic viscosity such that

$$\mu^* = [T^*(\tau - 1) + 1.0]^{\frac{3}{2}}\left(\frac{1 + \frac{S_\mu}{T_\infty}}{(T^*(\tau - 1) + 1.0) + \frac{S_\mu}{T_\infty}}\right), \tag{5}$$

k^* is the dimensionless thermal conductivity of fluid such that

$$k^* = [T^*(\tau - 1) + 1.0]^{\frac{3}{2}}\left[\frac{1 + \frac{S_k}{T_\infty}}{(T^*(\tau - 1) + 1.0) + \frac{S_k}{T_\infty}}\right] \tag{6}$$

and t^* is the dimensionless time (tU_0/D). τ ($\equiv T_w/T_\infty$) is the overheat ratio of hot wire.

One may note that both μ^* and k^* are based on Sutherland Formula (White (1991)) which expresses how the physical properties of the fluid changes with temperature as reflected in the overheat ratio of the hot wire (τ). S_μ and S_k are effective temperatures called the Sutherland constants, which are characteristic of the gas. For air, S_μ and S_k are taken as constants at 111 K and 194 K, respectively.

Eqs. (1)–(3) reveal the dimensionless parameters affecting the flow field and heat transfer characteristic as Reynolds number $\left(Re \equiv \frac{U_0 D}{\upsilon_\infty}\right)$, Prandtl number $\left(Pr \equiv \frac{\mu_\infty C_p}{k_\infty}\right)$, Grashof number $\left(Gr \equiv \frac{g\beta(T_w - T_\infty)D^3}{\upsilon_\infty^2}\right)$, and Eckert number $\left(Ec \equiv \frac{U_0^2}{C_p(T_w - T_\infty)}\right)$.

The instantaneous average Nusselt number is defined as:

$$Nu = \frac{1}{A_r}\oint \frac{qD}{k(T_w - T_\infty)}\mathrm{d}A_r = \frac{H'}{\pi k(T_w - T_\infty)} \tag{7}$$

where H' is the heat flux through the closed circulation which surrounds the cylindrical hot wire.

The corresponding dimensionless boundary conditions for Fig. 1 are given as follows:

$$B1: \quad x^* = x_s^* \equiv 0, \quad u^* = u_0^*, \quad v^* = 0, \quad T^* = T_\infty^* \equiv 0$$
$$B2: \quad y^* = H^*, \quad u^* = u_0^*, \quad v^* = 0, \quad T^* = T_\infty^* \equiv 0$$
$$B3: \quad y^* = 0, \quad u^* = u_0^*, \quad v^* = 0, \quad T^* = T_\infty^* \equiv 0$$
$$B4: \quad x^* = x_e^*, \quad \partial u^*/\partial x^* = \partial v^*/\partial x^* = 0, \quad \partial T^*/\partial x^* = 0$$
$$B5: \quad u^* = v^* = 0, \quad T^* = T_{\text{wire}}^* = 1$$

where

$$u_0^* = 1.0 + A\sin(2\pi Sc * t^*) \tag{8}$$

and

$$Sc = \frac{f}{f_0} = \frac{fD^2}{Re\upsilon_\infty}. \tag{9}$$

Here Sc is the dimensionless frequency of imposed streamwise velocity fluctuation where f is the associated imposed fluctuating frequency and A is the corresponding dimensionless amplitude of the imposed streamwise velocity fluctuation. As such,

$$f_0 \equiv \frac{Re\upsilon_\infty}{D^2} \tag{10}$$

is a reciprocal time scale.

3. Numerical calculations: grid distribution and size of computational domain

The time derivative was discretized using second-order, backward difference; and an implicit time scheme was employed to evaluate the spatial variables at the next time

level. For the spatial discretization of governing Eqs. (1)–(3), the finite volume method with a colocated arrangement of the variables was employed. Eqs. (2) and (3) were integrated over each control volume, leading to a balance equation for the fluxes through the control volume faces and the volumetric sources. As the fluid properties in Eqs. (2) and (3) were not treated as being constant, they were calculated as functions of temperature and updated at each new iteration. The diffusion contributions to the fluxes were evaluated using a second order central differencing scheme, while the convection contributions to the fluxes were evaluated using the second order upwind differencing scheme to reduce the effects of numerical diffusion on the solution. For the pressure calculation, a pressure correction equation was used instead of Eq. (1) and was solved iteratively with Eq. (2) following the SIMPLEC algorithm (Vandoormaal and Raithby (1984)). Convergence criteria were achieved when the maximum of the normalized absolute residuals in all equations is reduced to a value below 10^{-6}. Details of the numerics and implementation are available in the works of Li (2005) and Patankar (1980).

The whole computational domain was divided into several blocks, and was discretized with a different mesh density in different local blocks. In particular, surrounding the wire, the control volumes are much finer and are closely aligned with the flow direction so that numerical diffusion is reduced to a relatively low level based on the following analysis (see Section 3.1).

3.1. Grid distribution

The grid system used in the present study is shown in Fig. 2. The grid is distributed such that it minimizes numerical diffusion. Firstly, the grid lines have good orthogonality to decrease possible numerical diffusion. Secondly, locally refined grids around the cylinder were employed to improve the accuracy of the numerical results and to optimize the utilization of computational resources and, more importantly, to obtain better resolution of the flow field near the cylinder. The grids were deployed as such based on the analysis below.

For a two-dimensional flow, the numerical diffusion is given by De Vahl Davis and Mallinson (refer to Patankar, 1980) as,

$$\mu_{\mathrm{f}} = \frac{\rho U' \Delta x \Delta y \sin 2\theta}{4(\Delta y \sin^3\theta + \Delta x \cos^3\theta)} \tag{11}$$

where μ_{f} is the false diffusion coefficient, U' is the local velocity magnitude, θ is the angle between velocity direction and streamwise grid coordinate direction. Based on Eq. (11), the maximum ratio of numerical diffusion over the fluid viscosity $\frac{\mu_{\mathrm{f}}}{\mu}$ can be expressed as (assuming a maximum $\theta = 45^\circ$ and $\Delta x = \Delta y$)

$$\left(\frac{\mu_{\mathrm{f}}}{\mu}\right)_{\max} = \frac{\rho U' \Delta x \Delta y \sin 2\theta}{4(\Delta y \sin^3\theta + \Delta x \cos^3\theta)\mu} \approx \frac{\sqrt{2}}{4}\frac{\rho U' \Delta x}{\mu} = \frac{\sqrt{2}}{4} Re \times \Delta x^* \tag{12}$$

where Δx^* is the non-dimensional grid size based on the hot-wire diameter D.

From Eq. (11), it is necessary to keep the grid distribution closely aligned with the flow direction or decrease the grid size in the region where bigger angle θ exists. In all our simulations for the hot-wire application, the ratio of possible maximum false diffusion coefficient over the true viscous quantity is kept to be below 1% by ensuring the grid distribution was closely aligned with the flow direction and by the use of the small grid size in the region near the hot wire where possibly bigger angles θ may exist. For example, in the region around the hot wire, where the angle θ is not so close to zero, a much finer grid size was adopted. (Of course the angle θ is kept small due to our special 'eye' type grid distribution, as shown in Fig. 2). In this work, based on Eq. (12), there are 120 grid points around the hot wire of which

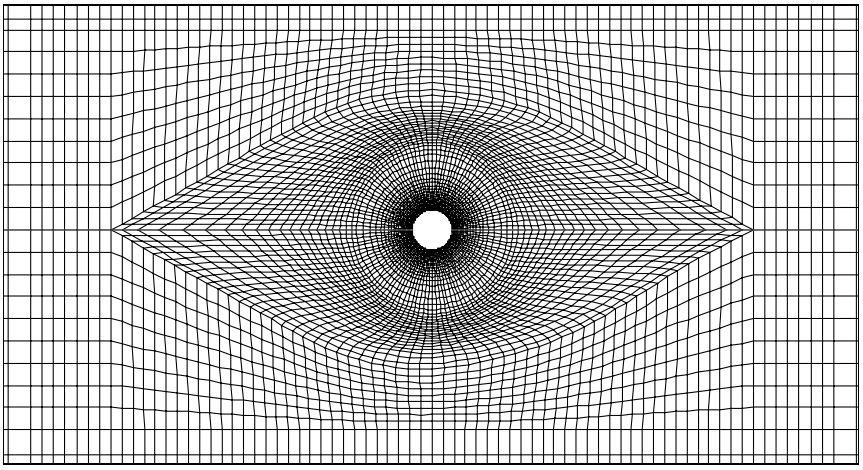

Fig. 2. The grid distribution around the hot wire.

details on the necessary grid independent check around the hot wire can be found in Li (2005).

Based on the above grid distribution and the minimum typical Reynolds number encountered in hot-wire measurement, the initial domain size of $20D \times 20D$ with the hot wire at the center was increased by adding new grid points in the outer region until the computed drag coefficient and Nusselt number were essentially invariant with the increase of the domain size. The test case was for Reynolds number $= 1.5 \times 10^{-2}$; the temperature of cylinder wall $T_w = 301$ K, and the temperature of free stream $T_0 = 300$ K. Correspondingly, the overheat ratio of hot wire (τ) was 1.003 so that the influence of temperature-dependent properties could be neglected. This allowed for direct comparison to the computed results of Lange (1997). The results obtained are given in Table 1.

From Table 1, we can see that as the computing domain increases, the result tends towards a converged solution. The differences of the drag coefficient and Nusselt number between the domains of $800D \times 800D$ and $1300D \times 1300D$ are 4.1% and 0.42%, respectively. For comparison, the drag coefficient and Nusselt number for a $4000D \times 4000D$ domain is also provided in Table 1. Lange (1997) has shown that the Nusselt number of a hot wire in an uniform flow computed based on domain size of order $4000D \times 4000D$ can be expressed as,

$$Nu = 0.082Re^{0.5} + 0.734Re^{x} \tag{13}$$

$$x = 0.05 + 0.226Re^{0.085}, \tag{14}$$

valid for the range of $10^{-4} \leqslant Re \leqslant 200$. Accordingly, the Nusselt number is 0.31627 for Reynolds number of 0.015. Compared with our Nusselt number of 0.31685 employing the same domain size, the difference is below 0.2%. More importantly, the results for the Nusselt number in Table 1 suggest that a computational domain size of $800D \times 800D$ (and larger) has led to an approximate asymptote for the calculated Nusselt number. A domain size of $1300D \times 1300D$ gives a reasonably good estimate with a difference of only about 0.1% from the quantity evaluated at the much larger domain of $4000D \times 4000D$. In this work, we shall use a domain size of $1300D \times 1300D$ for all the computations, unless otherwise stated.

Table 1
Variation of C_d and Nu with domain size for $Re = 1.5 \times 10^{-2}$

Case (n)	Domain size	Drag coefficient (C_d)	Nusselt number (Nu)
1	$20D \times 20D$	7.3089×10^2	0.41082
2	$100D \times 100D$	4.3401×10^2	0.33446
3	$200D \times 200D$	3.7049×10^2	0.32326
4	$400D \times 400D$	3.2617×10^2	0.32004
5	$800D \times 800D$	2.9798×10^2	0.31855
6	$1300D \times 1300D$	2.8617×10^2	0.31721
7	$4000D \times 4000D$	2.7838×10^2	0.31685

4. Heat transfer from a circular cylinder in uniform flow

Based on the grid distribution and computation domain size of $650D$ in the front, rear, top and bottom of the cylinder, the heat loss from a circular cylinder in uniform flow was computed at the low Reynolds number range normally encountered in equivalent near wall hot-wire measurements. For comparison, the results in terms of Nusselt number (N_{uf}, based on fluid properties evaluated at the film temperature defined as the mean of the upstream flow temperature and temperature on the hot wire) versus Reynolds number (Re_f, also based on fluid properties evaluated at the film temperature) at the overheat ratio of 1.5 are presented in Fig. 3 with Oseen's solution, Kramer's experimental formula (Kramers, 1946), and the (empirical) formula based on experiments by Collis and Williams (1959). The numerical predication of Lange et al. (1998) is also included. Our results agree reasonably well with Oseen's solution for Reynolds number less than 0.025, but the deviation increases with increasing Reynolds number for $Re_f \geqslant 0.025$; this deviation can be attributed to the failure/limitation of the linear assumption in Oseen's solution, particularly at higher Re_f. Our results are lower than those given by Kramer's formula, and the differences may be caused by the three-dimensional effect encountered in experiments. When comparison is made with the formula of Collis and Williams (1959), our computed Nusselt number indicates only

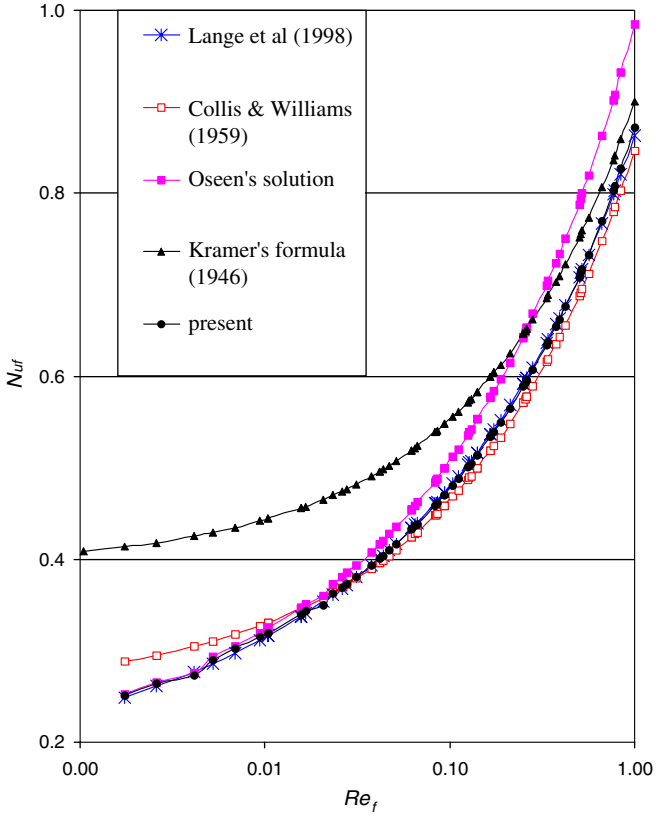

Fig. 3. Heat transfer from a circular cylinder in a freestream uniform flow for $\tau = 1.5$.

a slightly smaller quantity for $Re_f < 0.03$ and exhibits a slightly faster increase with $Re_f > 0.03$. In comparison with the result of Lange et al. (1998), our computed Nusselt number agrees very well, with only a very marginally higher value at the lower Reynolds number range. This small difference can perhaps be attributed to the neglect of the natural convection term in the simulation by Lange et al. (1998). It is suggested that at such low Reynolds number, natural convection becomes increasingly important. Overall, the reasonable agreement with experimental results augers well for the theoretical formulation and numerical method adopted in the present investigation.

Based on the above numerical simulation results of heat transfer from a circular cylinder in a steady flow, one can always obtain the calibration equation for the velocity (U_0, at the location of hot-wire centre) expressed in terms of Nu and then used it to evaluate the response to an imposed fluctuating velocity field (Section 5.4). (In experiments, the calibration equation for the velocity is expressed in terms of the electrical voltage E^2 across the hot wire which is proportional to Nu.) Additionally, the free stream calibration equation can be used as a reference against which subsequent calculations with wall effects are compared in order to obtain the near-wall corrections for various near-wall hot-wire measurements (see also Li et al. (2006)).

5. Heat transfer characteristics of the hot wire in fluctuating free stream flow

5.1. Comparison of the heat transfer of a hot wire placed in a free stream flow with and without imposed sinusoidal velocity fluctuation at Re = 150

In the experiment investigating flow field in the near wake of circular cylinder, Strouhal number is often used as a non-dimensional quantity to describe the vortex shedding frequency. It is defined as

$$S = \frac{D}{\tau_s U_\infty} \tag{15}$$

where τ_s is the period of the vortex shedding. It seems reasonable to define the characteristic frequency $f_0 \equiv \frac{U_\infty}{D} = \frac{Re\upsilon_\infty}{D^2}$ (Eq. (10)).

From Eqs. (10) and (15), Strouhal number can also be expressed as

$$S = \frac{D}{\tau_s U_\infty} = \frac{f_s * D^2}{Re * \upsilon_\infty} \tag{16}$$

where f_s ($\equiv 1/\tau_s$) is the frequency of vortex shedding.

We firstly want to compare the heat transfer characteristics of the hot wire in the free stream with and without the imposed fluctuation at a relatively high Reynolds number of 150 and a non-dimensional fluctuating frequency of 0.16. The two cases are calculated with an overheat ratio of 1.8. The first is a "hot wire" placed in a uniform free stream flow with $Re = 150$. (In the simulation of $Re = 150$, we set the diameter of hot wire at 2.25 mm and keep the flow velocity at 1.0 m/s so that flow is still regarded as incompressible. This is an artifice since the hot wire is typically of much smaller diameter and operating at a much lower Re of O(1) for velocity measurement. The selection of $Re = 150$ in this test is primarily aimed at comparison to published works on von Karman vortex shedding. All the other simulations at a much lower Re of O(1) were based on non-dimensional parameters which were in turn derived based on the normally used hot wire with a typical diameter size of 5 μm). Fig. 4 depicts the behavior of drag coefficient (C_d) on the cylinder for $Sc = 0.0$ (which corresponds to no imposed fluctuation) and the time history of Nusselt number (Nu) associated with the cylinder under the same flow condition. We can deduce from Fig. 4 that the condition as indicated by C_u and Nu has become periodic. One can see that there is periodic shedding of vortices from the cylinder into the downstream flow.

Konstantinidis et al. (2003) state that the fluctuations in the drag force on a cylinder in an uniform flow occur at twice the nominal shedding frequency due to the fact that each of the two alternating vortices that are shed during a cycle independently induces a fluctuating component.

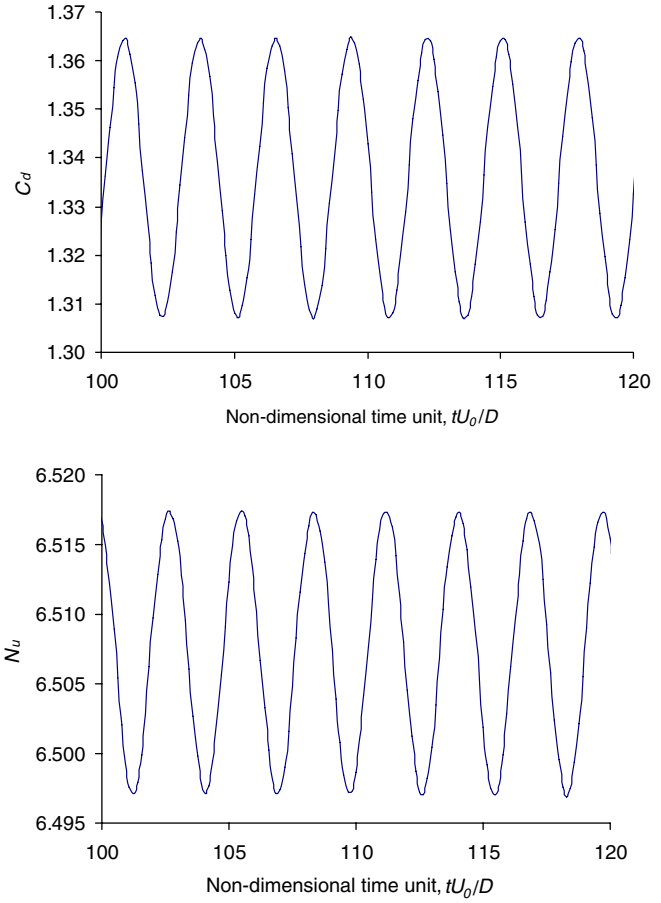

Fig. 4. Traces of drag coefficient (C_d) and surface Nusselt number (Nu) on cylinder for $Re = 150$ and $Sc = 0.0$.

From Fig. 4, we determine the fluctuating non-dimensional frequency for C_d and Nu as 0.356 which therefore corresponds to the nominal shedding frequency of Strouhal number identified as $S = 0.178$; this concurs with the experimental results of Gerrard (1978) obtained as 0.18. One may also take note of the findings by Braza et al. (1986) that the Strouhal number corresponding to the Reynolds number at 150 is 0.18. Furthermore, our Strouhal number at 0.178 is also in agreement with the empirical formula from Fey et al. (1998) to within 3%; the differences can possibly be attributed to the slight three-dimensional flow effects around the cylinder employed in the experiments.

Next, we simulate the same hot wire placed in a free stream flow with an imposed sinusoidal velocity fluctuation. The Reynolds number based on the mean velocity of incoming fluctuating flow is also set at 150. The amplitude ratio of the imposed streamwise velocity of fluctuation is $A = 0.6$ and the non-dimensional frequency $Sc = 0.16$ (which is equivalent to the fluctuating frequency of incoming flow at about 70 Hz). Fig. 5 depicts the traces of drag coefficient on the cylinder and the counterpart of the traces of Nusselt number. We can see from Fig. 5 that the respective traces have also become periodic.

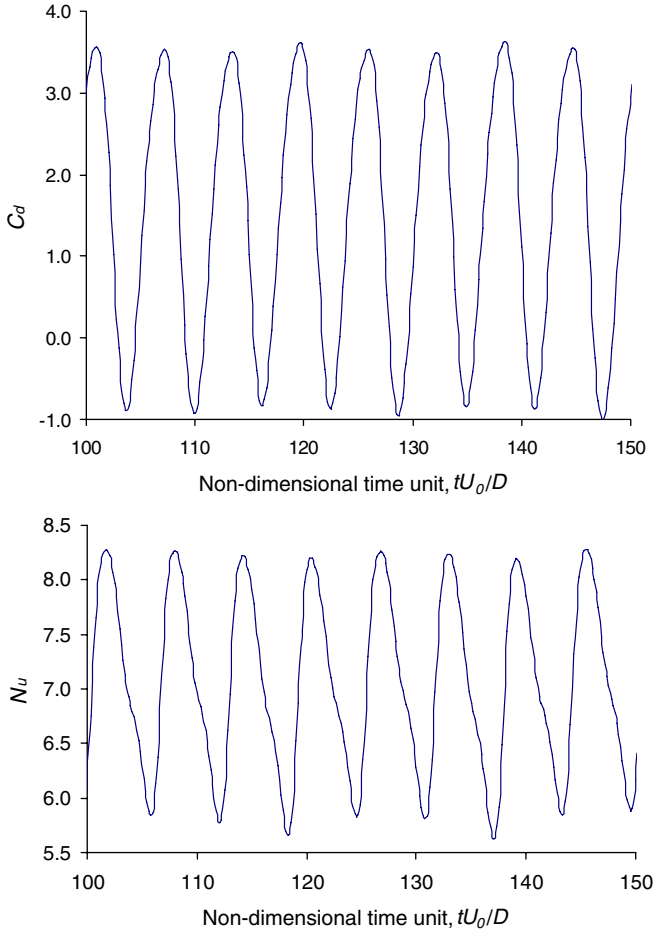

Fig. 5. Traces of drag coefficient (C_d) and surface Nusselt number (Nu) on cylinder for $Re = 150$ and $Sc = 0.16$.

We compare the calculated mean Nusselt number ($\overline{Nu}$) in one period taken from at least 10 cycles from Figs. 4 and 5, respectively. It is found that the averaged Nusselt number for flow with fluctuation is higher than that of the flow without imposed fluctuation (Nu_0); the ratio is about 1.08. That is to say the imposed fluctuation of incoming flow has led to a slight increase of the mean Nusselt number.

It is perhaps interesting to note that the (forced) shedding frequency from Figs. 4 and 5 gives rise to the Strouhal number of 0.08 which is precisely half the non-dimensional frequency ($Sc = 0.16$) of imposed fluctuating incoming flow. Although Barbi et al. (1986) observed that there is typically a range of perturbation frequencies, (f), around twice the natural Strouhal frequency in the unforced (unperturbed) wake, (f_v), where the vortex shedding frequency, (f_s), remains locked-on to precisely half the perturbation frequency, i.e., $f_s = f/2$ when $f/f_v \approx 2$, Griffin and Hall (1991) however pointed out that the range of frequency ratios, (f/f_v) over which lock-on occurs increases as the perturbation amplitude increases and is Reynolds number dependent. For our case we have, $Re = 150$, $\Delta u = 0.6$ m/s, $f = 70$ Hz, $d = 2.25 \times 10^{-3}$ m, thereby giving rise to the dimensionless amplitude $\varepsilon = \Delta u/(2\pi f d) = 0.61$. According to Konstantinidis et al. (2003), with a $\varepsilon = 0.61$, it is inferred that the limits of the lock-on range covers the value f/f_v of 1.0. Under this condition, the lock-on phenomenon probably occurs, where the vortex shedding frequency remains locked-on to precisely half the perturbation frequency; and this could have explained an increase of the mean heat transfer around the hot cylinder as noted earlier. It may be further noticed that there is a phase difference between C_d and Nu, which is close to 90°.

5.2. Heat transfer comparison between steady and fluctuating flows at various Sc and A = 0.6

Although the main objective of this study is to investigate the thermal response of a hot wire in a fluctuating free-stream flow in the range of Reynolds numbers typical for the hot-wire anemometer as used in near-wall measurements, i.e., $0.015 \leqslant Re \leqslant 1.5$, the limits of the computed range are extended up to 200 and with an overheat ratio of 1.8. This wider perspective for the variation of the investigated parameters of Nu with Reynolds number in the low Re regime (where the typical hot wire operates) can therefore be seen alongside the broader trend related to the higher Re regime (where most of other works can be found).

Fig. 6 gives the variation of the mean Nusselt number ratio ($\overline{Nu}/Nu_0$) with Reynolds number at various dimensionless oscillation frequency and $A = 0.6$. Here again Nu_0 is the Nusselt number corresponding to the steady flow imposed at the mean velocity. The abscissa is plotted in logarithmic scale so as to clearly depict the results in the low Reynolds number range where the usual hot-wire anemometer applies. In our computation, we have selected

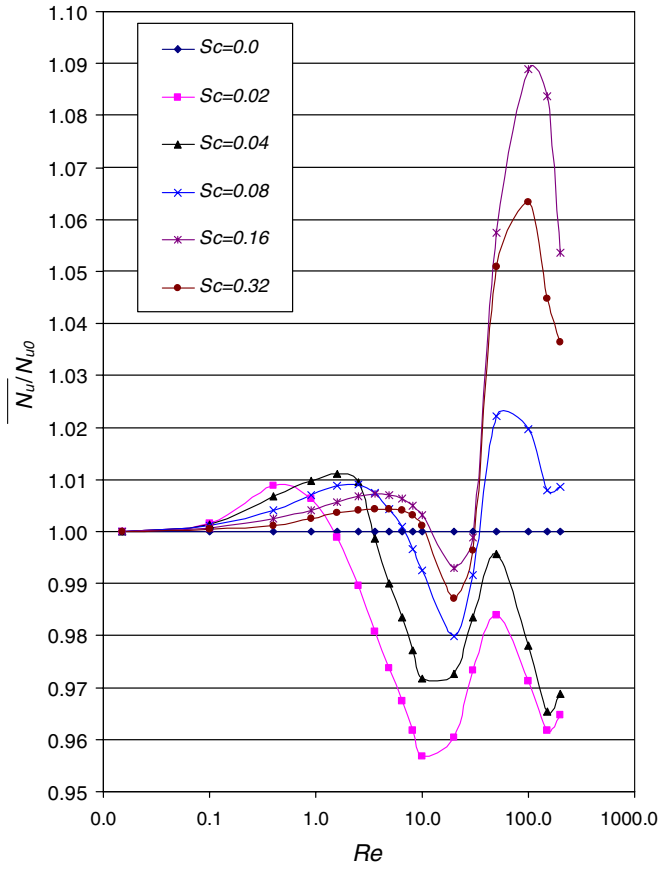

Fig. 6. Variation of Nusselt number ratio with Re at various Sc and $A = 0.6$.

$Re = 2.5 \times 10^{-2}$ as the typical lowest Reynolds number expected. As the typical fluctuating frequency in a turbulent air flow is about nominally in the 300–4500 Hz range, the associated range of Sc in the lower range of Re where hot-wire measurement is applicable is about 0.02–0.32.

From Fig. 6, it can be observed that for the range of Reynolds numbers tested the mean Nusselt number ratio is limited to between 0.95 and 1.10. It is interesting to note that the said ratio in the lower Reynolds number typically encountered in hot-wire measurement is significantly below ±5%. Therefore, this would imply that for any fluctuating flow measurement using a hot wire that had been calibrated under uniform free stream condition, it can be expected to yield a good result for the mean value. After all, the uncertainty associated with the calibration and among other factors for the hot wire is usually limited or taken to be conservatively about 5%.

5.3. Effects of amplitude ratio A on $(\overline{Nu}/Nu_0)$ at various Sc

To study the effect of amplitude ratio on $(\overline{Nu}/Nu_0)$, we computed for the flows at $Re = 0.1$, 0.9 and 2.5 as depicted in Figs. 7–9, respectively. The overheat ratio is set at 1.8. The amplitude ratio is set at $A = 0.05$, 0.1, 0.2, 0.4, 0.6 with

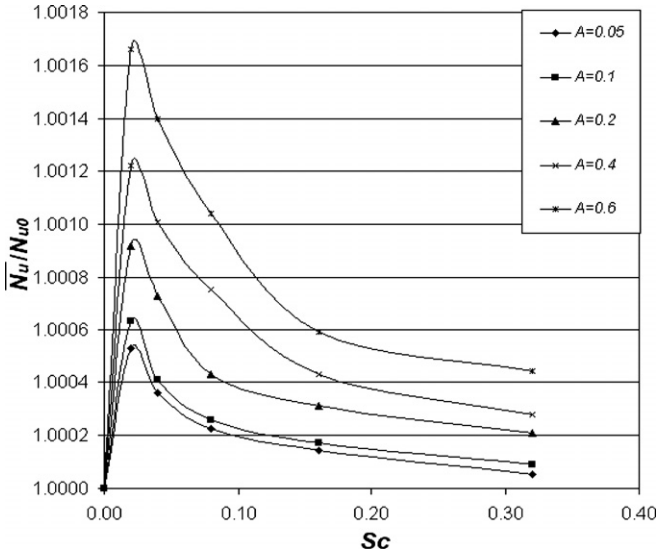

Fig. 7. Variation of Nusselt number ratio with Sc at various amplitude A and $Re = 0.1$.

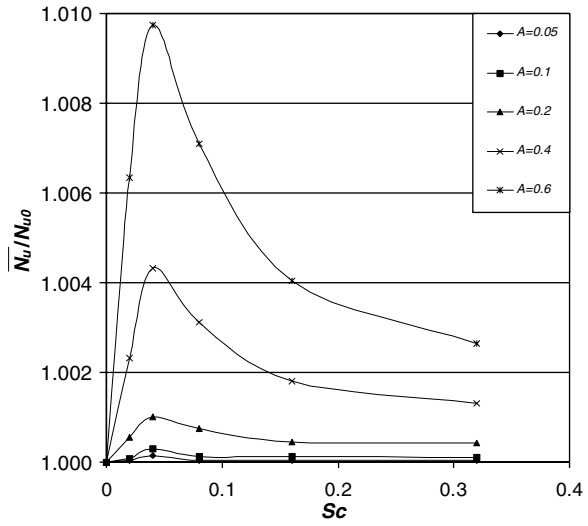

Fig. 8. Variation of Nusselt number ratio with Sc at various amplitude A and $Re = 0.9$.

$Sc = 0.02$, 0.04, 0.08, 0.16 and 0.32. Fig. 7 broadly suggests a possible maximum $\overline{Nu}/Nu_0$ occurring in the vicinity of $Sc \approx 0.02$ and the magnitude of this ratio is limited to less than about 1.002. Fig. 8, for the higher Re of 0.9, indicates a similar trend for $\overline{Nu}/Nu_0$ versus Sc. On comparing to Fig. 7, the maximum $\overline{Nu}/Nu_0$ occurs at the higher value of $Sc \approx 0.04$ and the largest magnitude is higher at less than 1.01. The plot of $\overline{Nu}/Nu_0$ against Sc for $Re = 2.5$ is shown in Fig. 9 and although the trend is quite different from those seen for the previous two lower Reynolds numbers, the respective amplitude ratio of $A = 0.05$, 0.1, 0.2, 0.4 and 0.6 indicates similar characteristics and the maximum variation of $\overline{Nu}/Nu_0$ lies between 0.99 and 1.01. Common among the three figures (Figs. 7–9) is that the $\overline{Nu}/Nu_0$ for $A = 0.6$ indicates the largest (absolute) deviation from

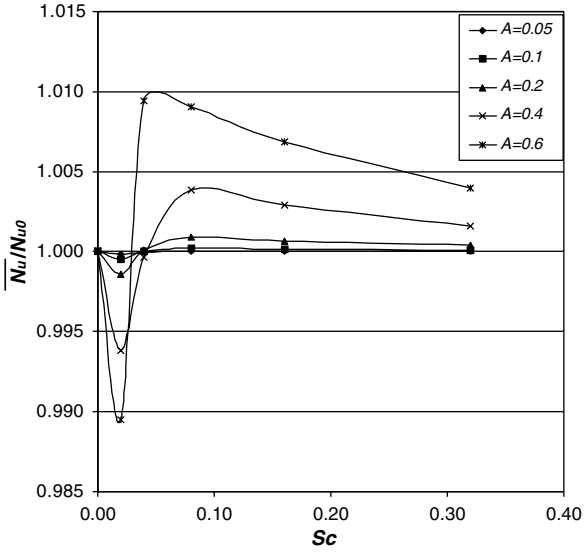

Fig. 9. Variation of Nusselt number ratio with Sc at various amplitude A and $Re = 2.5$.

unity against Sc. This has the important implication that the results shown in Fig. 6 for $A = 0.6$ would represent the maximum variation of $\overline{Nu}/Nu_0$ versus Sc compared to the other amplitude ratios less than 0.6. From these three figures, it suggests that operating the hot-wire anemometer at lower Re by keeping the wire diameter as small as possible has the added advantage of ensuring the value of $\overline{Nu}/Nu_0$ is even closer to unity. Still, the variation of $\overline{Nu}/Nu_0$ at $Re = 2.5$ is well within $\pm 5\%$ of unity, which is nominally the accepted accuracy in hot-wire measurements. The results provide support for the continual use of the hot wire to measure the mean velocity of a fluctuating flow.

5.4. Frequency response of hot wire at different fluctuating frequency

Thus far, the results presented in Sections 5.2 and 5.3 have centered on the amplitude or mean quantity of the fluctuating Nusselt number in the comparison to Nu_0. To investigate further the frequency response of a hot wire, we impose a known fluctuating sine-wave on the incoming flow and then determine the time-varying thermal response of the hot wire.

The specific test case is for the mean Reynolds number of 0.9. The overheat ratio used is 1.8. The imposed pulsating amplitude ratio is 0.4 and the imposed fluctuating frequency (f_{imp}) is 4 Hz, 400 Hz, 4000 Hz and 10,000 Hz, respectively. The resultant Nusselt number variation with frequency is given in Fig. 10 from where it is apparent that with the increase of imposed frequency in the freestream, the trace of the Nusselt number exhibits almost no change, and the phase difference (drift) corresponding to different pulsating flow frequency is also very small.

To further verify that the hot wire can keep faithfully to the imposed fluctuating velocity, we transform the Nusselt

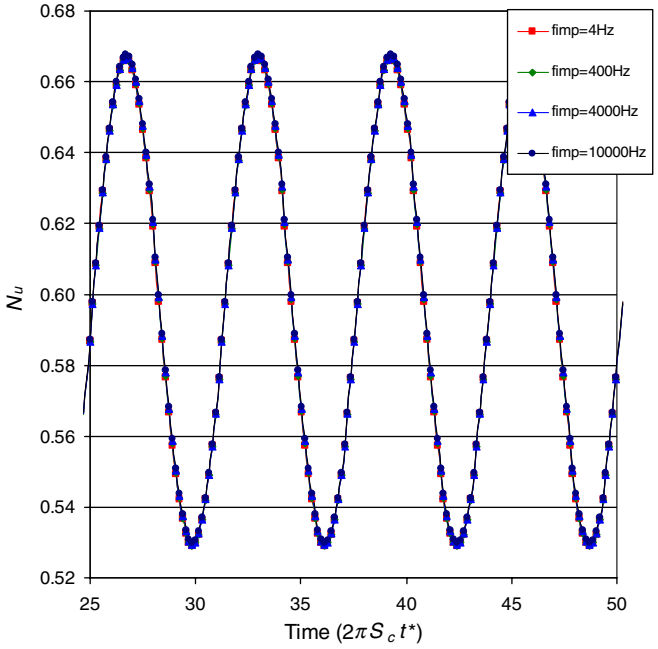

Fig. 10. Variation of Nu with frequency for freestream flow at $Re = 0.9$.

number to the corresponding velocity via the reference (mean) calibration curve (equivalent to Fig. 3). The (measured) velocity variation with frequency is given in Fig. 11 which shows the velocities corresponding to the imposed frequencies of 4 Hz, 400 Hz, 4000 Hz and

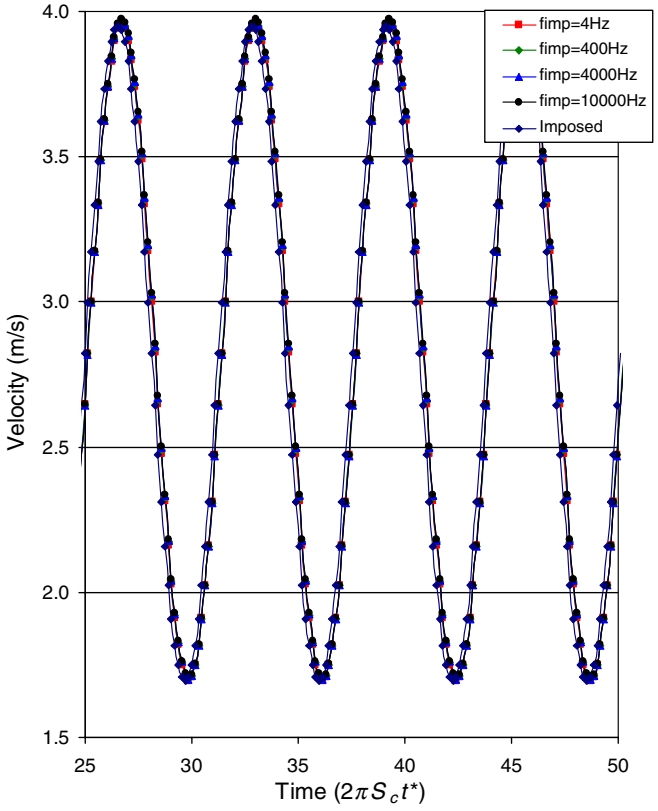

Fig. 11. Velocity variation with frequency for freestream flow at $Re = 0.9$.

10,000 Hz and the imposed known fluctuating velocity. It can be seen that the above five curves collapsed almost on top of each other, which implies that the hot wire can "measure" the imposed fluctuating velocity in the frequency range 0–10,000 Hz and with an amplitude range of 0–0.4. There is essentially very little or at most limited phase lag of below 2° between the imposed and measured velocities. This implies that the fast thermal response of a hot wire can keep up faithfully with the imposed fluctuating flow velocity in the frequency range of 0–10,000 Hz and the amplitude range of 0–0.4, which is quite typical of turbulent flow frequencies and turbulence intensities encountered in experiments. (Of course, for those turbulent flows where the mean quantity is very low compared to the magnitude of fluctuations, the measurement via hot-wire anemometer is not applicable and such cases are not considered here.)

It may be mentioned that Apelt and Ledwich (1979) have found that there is a not insignificant amplitude and phase difference between the computed Nu for a hot wire in a streamwise oscillating flow and the steady-state quantity evaluated via the imposed instantaneous value of Re. The calculation was carried out for only a single case of $Re = 10$. In other words, there is an amplitude and phase difference between the equivalent imposed velocity and (hot wire) measured velocity. This seeming discrepancy between the findings of Apelt and Ledwich and ours can be attributed to several factors. The computations in Apelt and Ledwich were carried out assuming constant fluid properties of viscosity and density, and the effects of buoyancy were neglected. As such, the overheat ratio (or temperature loading) of the hot wire was not considered, which is contrary to what is observed in experiments (see Collis and Williams (1959), Krishnamoorthy et al. (1985) or Chew et al. (1998b)). Another factor is the employment of convergence criterion as deduced to be 10^{-4} in Apelt and Ledwich which may not be sufficiently stringent. It has been shown recently in Li et al. (2006) that a convergence criterion of 10^{-6} is required and this was used to explain the discrepancy between the work of Chew and Shi (1993) and Lange et al. (1999) in the observed trend for the behaviour of a hot wire placed near an adiabatic wall. Chew and Shi had utilised the supposedly insufficiently stringent criterion of 10^{-4} in their numerical simulations; when the convergence criterion of 10^{-6} is employed, a similar trend as found in Lange et al. is observed. Lastly, and perhaps most importantly, an estimate of their imposed frequency based on a 5 μm hot wire yields a value of approximately 800 kHz. This is definitely way above the typical frequency of turbulence in which the hot wire is employed for velocity measurement. Overall, care is needed, therefore, in interpretating the computed results of Apelt and Ledwich (1979).

Finally, Table 2 gives the variation of the associated statistical quantities of the resultant streamwise velocity with imposed frequency; the statistical quantities calculated are the mean value, root mean square, and the kurtosis as normalized by the corresponding imposed known statistical quantities. As the imposed statistical quantities for skewness are zero, the calculated skewness is normalized by the skewness corresponding to the imposed frequency of 4 Hz. (One may note that these are typical statistical quantities commonly employed to characterize the turbulence in a quantitative manner for comparison, or to describe the turbulence as found for example in Fernholz and Warnack (1998) or Khoo et al. (2000) for the near-wall turbulent shear flow.) Table 2 clearly shows that all the above mentioned normalized statistical quantities are kept well below 1.05; in fact these values have a variation of less than 1% from unity. That is, the hot wire can measure the fluctuating velocity faithfully in terms of the turbulence statistics. Although the results presented here are for $Re = 0.9$, the characteristic features and behavior including the magnitude discussed above are equally valid for $Re \leqslant 2.5$ (not shown). Again, these are within the typical of Re encountered for hot-wire measurements under operating wall-remote conditions.

Table 2
Normalized statistic quantities versus frequency for mean flow $Re = 0.9$

Frequency (Hz)	Mean value	Root mean square	Skewness	Kurtosis
4	1.000342	1.000202	1	1.000498
400	1.000894	1.000381	1.000960	1.000965
4000	1.004152	1.001604	1.001750	1.002711
10,000	1.005636	1.002335	1.002847	1.003876

6. Conclusions

The comparison of hot-wire heat transfer characteristics in a uniform free stream flow and a streamwise fluctuating free stream flow was conducted to investigate the hot-wire thermal response. The imposed fluctuating free stream velocity is composed of a mean value and a sinusoidal oscillating component. The ranges of the parameters considered in this study are $0.025 \leqslant Re \leqslant 200$, $0 \leqslant Sc \leqslant 0.32$ and $A \leqslant 0.6$. The following conclusions could be drawn from the present study:

1. For any fluctuating flow, a hot wire having been calibrated under imposed mean free stream condition can be used for the measurement of mean velocity quantity (and higher order of turbulence statistics). The deviation of the mean Nusselt number ratio ($\overline{Nu}/Nu_0$) from unity is limited to less than ±5%. In the lower Re range of $Re \leqslant 1.0$, the said ratio deviation from 1.0 is kept well below ±1%.
2. The very rapid thermal response of the hot wire has enabled the faithful measurement of fluctuating velocity in the typical range of frequency of $0 \leqslant f \leqslant 10{,}000$ Hz and amplitude ratio of $A \leqslant 0.4$ encountered in a turbulent flow. There is essentially very little or limited phase lag between the imposed and measured fluctuating velocities.

Acknowledgements

We wish to acknowledge Professor P. Freymuth from University of Colorado, Boulder for the discussions we had, the interest he has shown in this work and the advice he has given.

References

Apelt, C.J., Ledwich, M.A., 1979. Heat transfer in transient and unsteady flows past a heated circular cylinder in the range $1 \leqslant Re \leqslant 40$. J. Fluid Mech. 95, 761–777.

Barbi, C., Favie, D.P., Maressa, C.A., Telionis, D.P., 1986. Vortex shedding and lock-on of a circular cylinder in oscillatory flow. J. Fluid Mech. 170, 527–544.

Bearman, P.W., Downie, M.J., Graham, J.M.R., Obaasaju, E.D., 1985. Forces on cylinders in viscous oscillatory flow at low Keulegan–Carpenter numbers. J. Fluid Mech. 154, 337–356.

Braza, M., Chassaing, P., Minh, H.H., 1986. Numerical study and physical analysis of the pressure and velocity fields in the near wake of a circular cylinder. J. Fluid Mech. 165, 79–130.

Cheng, C.H., Chen, H.N., Aung, W., 1997a. Experimental study on the effect of transverse oscillation on convection heat transfer from a circular cylinder. J. Heat Transfer 119, 474–482.

Cheng, C.H., Hong, J.L., Aung, W., 1997b. Numerical prediction of lock-on effect on convective heat transfer from a transversely oscillating circular cylinder. Int. J. Heat Mass Transfer 40, 1825–1834.

Chew, Y.T., Shi, S.X., 1993. Wall proximity influence on hot-wire measurements. In: So, R.M.C., Speziale, C.G., Launder, B.E. (Eds.), Near-Wall Turbulent Flows. Elsevier, Amsterdam, pp. 609–619.

Chew, Y.T., Khoo, B.C., Lim, C.P., Teo, C.J., 1998a. Dynamic response of hot-wire anemometer. Part II: A flushed mounted hot-wire and hot-film probes for wall shear stress measurements. Meas. Sci. Technol. 9, 764–778.

Chew, Y.T., Khoo, B.C., Li, G.L., 1998b. An investigation of the wall effects on hot-wire measurements using a bent sublayer probe. Meas. Sci. Technol. 9, 67–85.

Collis, D.C., Williams, M.J., 1959. Two-dimensional convection from heated wires at low Reynolds numbers. J. Fluid Mech. 6, 357–384.

Fernholz, H.H., Warnack, D., 1998. The effects of a favourable pressure gradient and of the Reynolds number on an incompressible axisymmetric turbulent boundary layer. Part 1. The turbulent boundary layer. J. Fluid Mech. 359, 329–356.

Fey, U., Koenig, M., Eckelmann, H., 1998. A new Strouhal–Reynolds-number relationship for the circular cylinder in the range $47 < Re < 2 \times 10^5$. Phys. Fluids 10, 1547–1549.

Gerrard, J.H., 1978. The wakes of cylindrical bluff bodies at low Reynolds number. Philos. Trans. Roy. Soc. A 288, 351–382.

Griffin, O.M., Hall, M.S., 1991. Vortex shedding lock-on and flow control in bluff body wakes – review. ASME J. Fluids Eng. 113, 526–544.

Gundappa, M., Diller, T.E., 1991. The effects of free-stream turbulence and flow pulsation on heat transfer from a cylinder in crossflow. J. Heat Transfer 113, 766–769.

Hegge Zijnen, B.G.V.D., 1958. Heat transfer from horizontal cylinders to a turbulent air flow. Appl. Sci. Res. A7, 205–223.

Honji, H., 1981. Streaked flow around an oscillating circular cylinder. J. Fluid Mech. 107, 509–520.

Iliadis, G., Anagnostopoulos, P., 1998. Viscous oscillatory flow around a circular cylinder at low Keulegan–Carpenter numbers and frequency parameters. Int. J. Numer. Methods Fluids 26, 403–442.

Justesen, P., 1991. A numerical study of oscillatory flow around a circular cylinder. J. Fluid Mech. 222, 157–196.

Kezios, S.P., Prasanna, K.V., 1966. Effect of vibration on heat transfer from a cylinder in normal flow. ASME Paper no. 66-WA/HT-43.

Khoo, B.C., Chew, Y.T., Lim, C.P., Teo, C.J., 1998. Dynamic response of hot-wire anemometer. Part I: A marginally elevated hot-wire probe for near-wall velocity measurements. Meas. Sci. Technol. 9, 751–763.

Khoo, B.C., Chew, Y.T., Teo, C.J., Lim, C.P., 1999. The dynamic response of hot-wire anemometer. Part III: Voltage-perturbation versus velocity perturbation testing for near-wall hot-wire/film robes. Meas. Sci. Technol. 10, 152–169.

Khoo, B.C., Chew, Y.T., Teo, C.J., 2000. On near-wall hot-wire measurements. Exp. Fluids 29, 448–460.

Konstantinidis, E., Balabani, S., Yianneskis, M., 2003. The effect of flow perturbations on the near wake characteristics of a circular cylinder. J. Fluids Struct. 18, 367–386.

Kramers, K., 1946. Heat transfer from spheres to flow media. Physica 12, 61–80.

Krishnamoorthy, L.V., Wood, D.H., Antonia, R.A., Chambers, A.J., 1985. Effects of wire diameter and overheat ratio near a conducting wall. Exp. Fluids 3, 121–127.

Lange, C.F., 1997. Numerical predications of heat and momentum transfer from a cylinder in crossflow with implications to hot-wire anemometry. Ph.D. Thesis, University of Erlangen-Nurnberg, Erlangen, Germany.

Lange, C.F., Durst, F., Breuer, M., 1998. Momentum and heat transfer from cylinders in laminar crossflow at $10^{-4} \leqslant Re \leqslant 200$. Int. J. Heat Mass Transfer 41, 3409–3430.

Lange, C.F., Durst, F., Breuer, M., 1999. Wall effects on heat losses from hot-wires. Int. J. Heat Fluid Flow 20, 34–47.

Leung, C.T., Ko, N.W.M., Ma, K.H., 1981. Heat transfer from a vibrating cylinder. J. Sound Vibration 75, 581–582.

Li, J.D., 2004. Dynamic response of constant temperature hot-wire system in turbulence velocity measurements. Meas. Sci. Technol. 15, 1835–1847.

Li, W.Z., 2005. Numerical simulations of heat transfer of hot-wire anemometer. Ph.D. Thesis, National University of Singapore.

Li, W.Z., Khoo, B.C., Xu, D., 2006. The thermal characteristics of a hot wire in a near-wall flow. Int. J. Heat Mass Transfer 49, 905–918.

Obasaju, E.D., Bearman, P.W., Graham, J.M.R., 1988. A study on forces, circulation and vortex patterns around a circular cylinder in oscillatory flow. J. Fluid Mech. 196, 467–494.

Patankar, S.V., 1980. Numerical Heat Transfer and Fluid Flow. McGraw-Hill.

Perry, A.E., Morrison, G.L., 1971. Static and dynamic calibrations of constant-temperature hot-wire systems. J. Fluid Mech. 47, 765–777.

Saxena, U.C., Laird, A.D.K., 1978. Heat transfer from a cylinder oscillating in a cross-flow. J. Heat Transfer 100, 684–689.

Shi, J.M., Gerlach, D., Breuer, M., Biswas, G., Durst, F., 2004. Heating effect on steady and unsteady horizontal laminar flow of air past a circular cylinder. Phys. Fluids 16, 4331–4345.

Skomedal, N.G., Vada, T., Sortland, B., 1989. Viscous forces on one and two circular cylinders in planar oscillatory flow. Appl. Ocean Res. 11, 114–134.

Smith, P.A., Stansby, P.K., 1991. Viscous oscillatory flows around cylindrical bodies at low Keulegan–Carpenter numbers using the vortex method. J. Fluids Struct. 5, 339–361.

Vandoormaal, J.P., Raithby, G.D., 1984. Enhancements of the SIMPLE method for predicating incompressible fluid flows. Numer. Heat Transfer 7, 147–163.

White, F.M., 1991. Viscous Fluid Flow. McGraw-Hill, New York.